Submicronic calcite particles with controlled morphology tailored by polymer skeletons *via* carbonation route with compressed or supercritical CO_2†

Wei Li, Qisi Yu and Peiyi Wu*

Received 17th June 2009, Accepted 20th July 2009
First published as an Advance Article on the web 6th August 2009
DOI: 10.1039/b914787j

The preparation of biominerals based on CO_2 fixation and regulatory effect of organic macromolecules has attracted more and more interests in recent years, inspired by the increase in technological interests in bio-inspired materials science and fabrication of useful products *via* an environmentally friendly process. In this paper, submicronic $CaCO_3$ particles with ellipsoidal morphology were synthesized using compressed or supercritical CO_2 with sodium salt of carboxymethyl cellulose (NaCMC) as a template. By regulating some experimental parameters, including the concentration and molecular weight of NaCMC, as well as the CO_2 pressure and temperature, the morphology and size of the $CaCO_3$ particles could be effectively controlled. Besides, in contrast to the effective results of another additive, Polyacrylic Acid (PAA), our research suggested that the morphology of the synthesized particles was strongly related to the flexibility of the polymer chains, namely, the relatively rigid chains induce the formation of ellipsoidal particles while the more flexible chains would result in the spherical ones. In addition, amorphous calcium carbonate was traced as an intermediate phase during the crystallization process. Based on the experimental results, we discussed the formation mechanism of such particles: the polymer chains serve as the skeletons, then the ions attach along the chains to grow. The final morphology of $CaCO_3$ aggregates is tailored by the flexibility of the polymer chain, while the size of the particles is related with the chain length of the polymer. In comparison with the traditional mineralization methods, here we provide a highly efficient and versatile approach to integrate the fixation of CO_2 and the regulating effect of different polymer chains, to produce submicroscopic $CaCO_3$ particles and further control their morphology and size distribution. Such an approach is facile and of potential importance as an environmentally benign industrial route to synthesize biomaterials, and it may also serve to shed light on the study of the mechanism of biomimetic mineralization.

Introduction

As an inorganic mineral, calcium carbonate is widely used by mankind for industrial applications[1] and by living organisms for important biological functions including protection and structural support.[2] In many industrial branches like paper-making, plastics, paints and cosmetics *etc.* the application of $CaCO_3$ particles has been growing fast,[3] in which control of the size, morphology and polymorph of the particles is among the most significant items,[4] due to the dependence of the involved materials properties, such as hardness, optical or mechanical properties on solid-state structure. It is widely accepted that $CaCO_3$ has three different anhydrous phases: vaterite, aragonite and calcite, with an increasingly thermodynamic stability.[2] In addition, the amorphous calcium carbonate (ACC), which plays a key role in the early stage of biogenic $CaCO_3$ and as an important precursor of the crystallized $CaCO_3$, has been greatly studied recently.[5-7]

Compared to the traditional fabrication methods of $CaCO_3$ like carbonization and metathesis, the newly-developed synthesis of $CaCO_3$ in compressed and supercritical CO_2 ($scCO_2$) provided an alternative technique which has recently attracted more and more attention.[1,3,4,8-10] Such an approach is very simple and highly efficient, because the properties of CO_2 could be easily adjusted by altering the temperature and pressure, which will facilitate the dissolution of CO_2/HCO_3^-, resulting in the rapid production of $CaCO_3$ particles in several hours. Furthermore, the new route shows great potential use in CO_2 sequestrations, which may suggest contributions to settle the problems of increased CO_2 emissions and global warming.[8] In previous work, we have utilized the unique properties of CO_2, including relatively high density and low viscosity, nearly no surface tension and high diffusivity, solubility and

---

Key Laboratory of Molecular Engineering of Polymers of Ministry of Education Laboratory of Advanced Materials Department of Macromolecular Science, Fudan University, Shanghai, 200433, P. R. China. E-mail: peiyiwu@fudan.edu.cn

† Electronic supplementary information (ESI) available: TGA curves of $CaCO_3$ particles obtained under different conditions. See DOI: 10.1039/b914787j

plasticizing actions in polymers,[11-13] to propose a novel approach to prepare hybrids based on cellulose and titania,[14] and to induce the fast transition of crystal phase of isotactic Poly-1-butene.[15]

There have been some reports focusing on the fabrication of $CaCO_3$ with the utilization of compressed CO_2 or $scCO_2$, in order to explore an optimized route to improve the productivity and modify the morphology and size of $CaCO_3$ without addition of organic additives.[1,3,4,9] However, reports on mineralization of $CaCO_3$ in compressed or $scCO_2$ under control of organic additives or templates are relatively few.[8,10,16] To determine whether different additives cause diverse results in control of $CaCO_3$ morphology, Han[10] *et al.* used three kinds of surfactants to prepare $CaCO_3$ by carbonation route in compressed CO_2 and $scCO_2$, with a conclusion that the binding ability of the surfactants to crystal faces of $CaCO_3$ was different, which might induce unique effects on the growth of $CaCO_3$ crystals. Wakayama[8,16] *et al*. fabricated $CaCO_3$ thin films by biopolymers (*e.g.* cellulose or chitosan) from aqueous solutions with calcium acetate and polyacrylic acid (PAA) in $scCO_2$, and different yields and compositions of $CaCO_3$ was accounted to the different levels of PAA adsorbed to the macromolecules. Recently Aymonier and Cansell *et al.*[17,18] developed a novel approach to synthesize functional organic–inorganic nanoparticles with polymer templates mediated by supercritical CO_2, like palladium and silver nanoparticles. Besides, the CO_2-in-water emulsion template was also used to synthesize hollow silica spheres,[19,20] silver halide nanoparticles,[21] CdS and ZnS nanoparticles.[22]

We have studied the influence of an ionic ether of cellulose, carboxymethyl cellulose (CMC), on the morphology, polymorph and size of $CaCO_3$ using the CO_2-diffused method and discussed the possible mechanism.[23] Herein, we compare the different formation process and mechanism between the traditional mineralization method and the new method with compressed and supercritical CO_2. To our knowledge expand, the final submicroscopic calcite particles in size of several hundreds of nanometres have not been often reported yet. In our opinion, the combination of the compressed and supercritical CO_2 method and the control of organic additives may not only provide a novel method to fabricate industrially refined $CaCO_3$ particles, but also probably inspire a brand-new view angle to the investigation of the mechanism of biomimetic mineralization.

Experimental

Materials

Calcium hydroxide ($Ca(OH)_2$) and polyacrylic acid (PAA, M_w = 2000) were purchased from Sinopharm Chemical Reagent Co. Ltd. The two kinds of sodium salts of carboxymethyl cellulose (NaCMC) were both purchased from Acros with a molecular weight (M_w) of 90 000 and 700 000, and degree of carboxyl substitution (DS) of 0.7 and 0.9, respectively. All reagents were of analytical grade and used without further purification. CO_2 with a purity of 99.9% was purchased from Shanghai Jifu Gas Co. Ltd. The water used in the experiments is deionized water (DIW).

Synthesis of $CaCO_3$ particles

All glassware (glass bottles and small pieces of glass substrates) was cleaned and sonicated in ethanol for 15 minutes, then rinsed with DIW, further soaked in a HNO_3-H_2O_2-DIW(1 : 1 : 1) solution, then rinsed with DIW, and finally dried with acetone. For a typical experiment, 0.03 g $Ca(OH)_2$ powder was dispersed in 10 ml NaCMC aqueous solution (1 g/l), and a piece of glass substrate was immersed in a 10 ml vessel with the above-mentioned suspension. The vessel was placed into an autoclave with a capacity of 40 ml. Afterwards, the autoclave was sealed, into which CO_2 was charged until a certain pressure. Then the autoclave was immediately put into the water bath to a certain temperature. (For the compressed condition, the pressure is 5 MPa and the temperature is 20 °C; for supercritical condition, the pressure is 8 MPa and the temperature is 45 °C.) After different periods of reaction time, CO_2 was released slowly and the glass piece was taken out and dried at ambient temperature and in vacuum conditions for further examination.

Characterization

The Transmission Electron Microscope (TEM) images were taken with a JEOL JEM 2011 at 200 KV equipped with electron diffraction. Scanning Electron Microscope (SEM) observations were performed on a TS5136MM microscope with gold coated. X-Ray powder diffraction (XRD) data were recorded on an X'pert Pro with Cu K_α radiation. Thermogravimetric analysis of the powder was carried out on a Perkin-Elmer Pyris-1 TGA to determine the contents of organic additives.

Results and discussion

Effect of NaCMC concentration on the morphology of $CaCO_3$ particles

Crystallization process of $CaCO_3$ was performed in the presence of NaCMC firstly with a molecular weight of 90 000 as the organic additive in compressed CO_2 to study the effect of polymer concentration. The SEM images of the particles obtained under different polymer concentrations were presented in Fig. 1. We can see from Fig. 1a that after 10 min reaction under the 0.1 g/l polymer concentration nearly ellipsoidal particles were obtained, with a size of approximately 300–500 nm but the size distribution was not quite uniform. Fig. 1b shows the products obtained after 60 min reaction under the same concentration, most of which revealed an ellipsoidal morphology and a size of 300–600 nm, similar to those produced in 10 min reaction, which suggested, to some extent, that the reaction in the autoclave is so fast that it is not easy to tell the difference between the particles yielding in 10 min and 60 min, that is to say, the rate of the reaction is so fast that it is nearly completed in a 10 min interval.

Fig. 1c shows the SEM image of $CaCO_3$ particles under 1 g/l polymer concentration after 10 min reaction. The particles depict ellipsoidal shape with a size about 300 nm. After 60 min reaction, both the size and the morphology of the particles (Fig. 1d) are almost unchanged while the size distribution is nearly mono-dispersed. In the enlarged picture (Fig. 1e), we can estimate that the aspect ratio of the ellipsoid is about 2 : 1. When the polymer concentration was increased to 10 g/l, as showed in

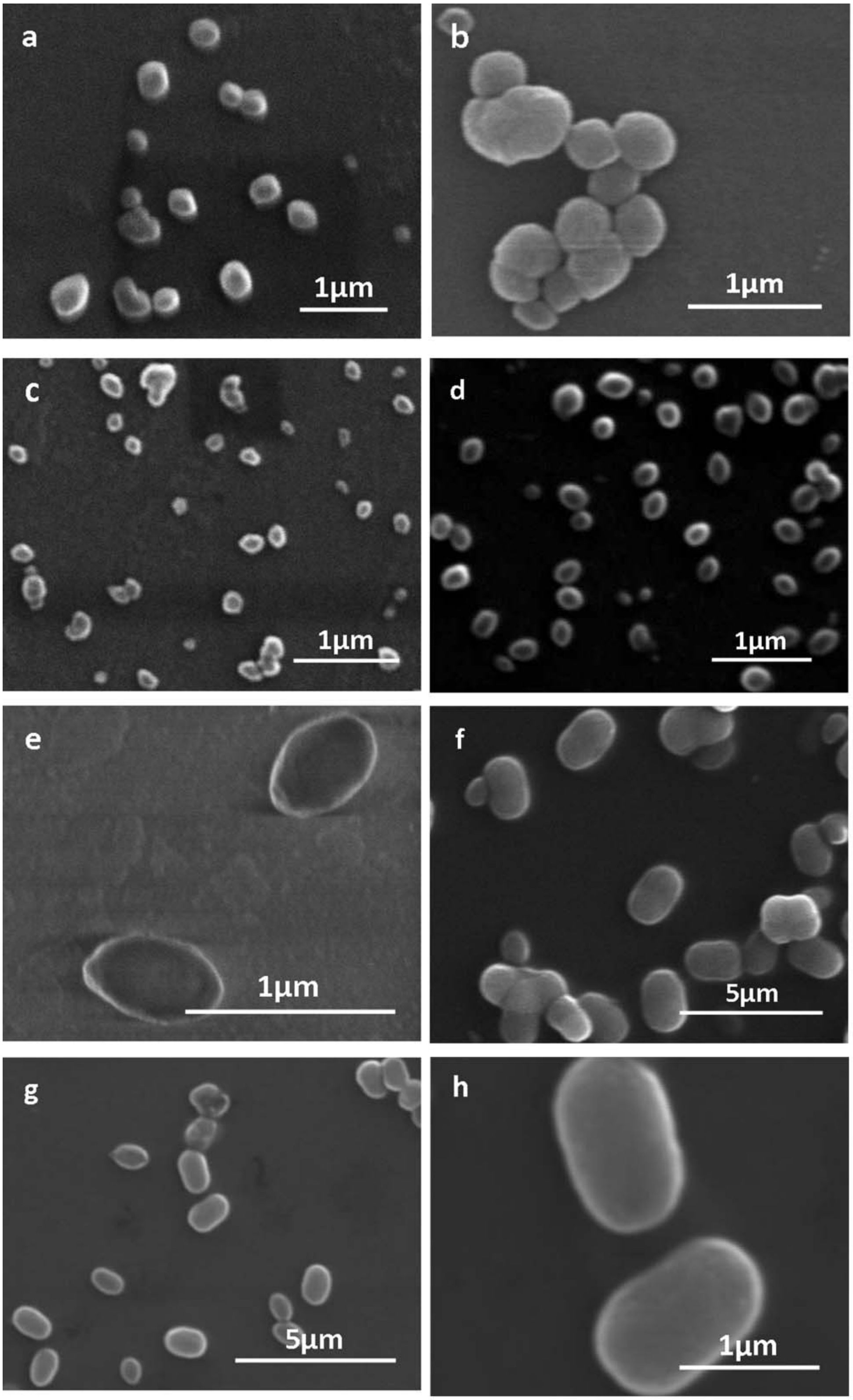

Fig. 1 SEM images of $CaCO_3$ particles obtained in 0.1 g/l(a), 1 g/l(c), 10 g/l(f) NaCMC and $Ca(OH)_2$ suspension after 10 min reaction and particles obtained in 0.1 g/l(b), 1 g/l (d, e), 10 g/l (g, h) NaCMC and $Ca(OH)_2$ suspension after 60 min reaction.

Fig. 1f, it is revealed that the ellipsoidal particles could be still obtained, but there are two significant points worth noting: first, the size of the particles increased to 1–2μm compared with the size of Fig. 1a and 1b (several hundreds of nanometres); second, the end of the ellipsoidal particles is more rounded, not so sharp as those obtained under 1 g/l concentration.

We further used TEM to investigate the structure of the particles we have obtained. Fig. 2a and Fig. 2b show the TEM images of $CaCO_3$ particles obtained under 1 g/l concentration after 10 min reaction. Interestingly, although we can just find ellipsoidal particles in the SEM images, we observe in the TEM images ellipsoidal or rounded particles with a size of 100–150 nm, in spite of the low numbers. The electron diffraction (ED) patterns performed on the particles show that the particles is amorphous calcium carbonate (ACC), which suggests that the final particles may go through an ACC intermediate phase. According to Addadi *et al.*[7] and Xu *et al.*,[24] ACC plays a key role as an important precursor in the biomineralization process and can transform into anhydrous crystalline phases quickly *via* a dissolution-recrystallization way. Moreover, in Fig. 2a and 2b, most of the ACC particles depict a depression in the center, as the red arrow indicates, which are probably due to the existing of skeletons of polymer chains in the center.

Fig. 2c shows the TEM image of $CaCO_3$ particles obtained under 1 g/l concentration after 60 min reaction, which depicts that the particle is ellipsoidal with a size of about 300 nm, consistent well with the SEM results. It is worth noting that there is no obvious depression in the center of the particle, suggesting that ACC has transited into crystalline phase and the inner part was getting dense with the growth process continuing. Fig. 2d is the high resolution TEM image of Fig. 2c and the d-spacing is 3.02 Å, corresponding to the (104) face of calcite, which is confirmed by the ED patterns (the inset of Fig. 2d).[25] Fig. 2e is a typical TEM image of the particle obtained under 10 g/l concentration after 60 min reaction. The particle is ellipsoidal with a more rounded end and the size is about 2 μm, in accordance with the SEM results.

The X-ray diffraction patterns (Fig. 3a–d) reveal that the polymorph of the particles obtained under different polymer concentrations and in different time intervals in compressed CO_2 is principally calcite, which is in agreement with the ED results. There are little amounts of vaterite, maybe controlled by the kinetic factors. The involvement of polymer chains is confirmed by TGA analysis (see Fig. S1–S3, ESI†). The content of organic additives in the $CaCO_3$ particles obtained under control of 0.1 g/l NaCMC is about 2.5% after both 10 min and 60 min reaction, further indicating that the rate of the reaction is so fast that the reaction is nearly completed within 10 min. The content of organic additives in the particles obtained under control of 1 g/l NaCMC is 6%, higher than the 0.1 g/l sample, which is reasonable due to the high polymer concentration.

To explore the general factors that determined the formation of such ellipsoidal particles, we go back to the conformation of the NaCMC chains in aqueous solution. According to Kamburova and Radeva,[26] the conformation of NaCMC chains is extent, which is like a rod and we listed some parameters of NaCMC solution in Table 1. We infer that the rigidity of the NaCMC chain is the origin of the formation of ellipsoidal particles. Simply, the NaCMC chains were taken as the skeletons, then calcium ions and CO_3^{2-} originated from CO_2 bubbles attached along the chain, followed by the formation of $CaCO_3$ grains. Because of the rigidity of the rod-like chains, the final products depicted ellipsoidal morphology.

Table 1 Some parameters in the NaCMC aqueous solution

Molar mass	Degree of substitution	Counter length(nm)	Root-mean-square end-to-end distance	Overlap concentration C*(g/l)
90,000	0.7	206	~160	0.71
700,000	0.9	~1000	>500	<0.1

The root-mean-square end-to-end distance of NaCMC chain with M_w of 90 000 is about 160 nm, which is consistent with the size of the particles obtained under 0.1 and 1 g/l (low concentration region) concentration. Besides, the overlapped concentration (C*) is *ca.* 0.71 g/l, so it is reasonable that when the polymer concentration is lower or close to the overlapped concentration, the skeletons of NaCMC exist mainly as rod-like single chains and thus induce the formation of ellipsoidal $CaCO_3$ particles in size of about 300 nm. While the polymer concentration is much higher than the overlapped concentration, the polymer chains overlapped severely. The intersected chains serve as templates for ions to attach and grow, thus the final particles embrace not a single chain but several chains so that their size increased to 1–2 μm and the end of particles became more rounded.

To the best of our knowledge, it is the first time to obtain such submicroscopic $CaCO_3$ particles with ellipsoidal morphology. Due to the convenience, low cost and high efficiency, this method may find great use in a lot of industrial aspects. In all, the polymer concentration has a significant effect on the morphology and the size of the $CaCO_3$ particles. Particles in small size of 300 nm yield at low concentrations and those in larger size of 1–2 μm yield at relatively high concentration. In the simple time-resolved experiment, we seize very little of intermediate ACC phase by TEM, which indicates that the formation of the final ellipsoidal calcite particles probably go through a dissolution–recrystallization process originated from ACC.

Effect of chain length of NaCMC

We used NaCMC with a larger molecular weight (700 000) to perform a comparison of the additive polymers with different chain length on the formation of $CaCO_3$ particles. Fig. 4a and 4b exhibit the SEM images of $CaCO_3$ particles obtained under 1 g/l NaCMC concentration. The particles are similar to those obtained under lower M_w except that the size of the particles is much larger (*ca.* 1.5 μm). According to our previous analysis, there are two causes: first, the overlapped concentration is much lower for the NaCMC solution with higher M_w (lower than 0.1 g/l, as Table 1 depicts), so even at 0.1 g/l, the chains have already overlapped, so it is several chains not a single chain that serve as templates, thus the final particles embrace several chains; second, the chain length of NaCMC with higher M_w is larger, thus, as the skeleton of the final particles, the polymer chains with larger size induces $CaCO_3$ particles with larger size. Fig. 4c and 4d depicts the particles obtained under 5 g/l NaCMC concentration. The morphology is also ellipsoidal

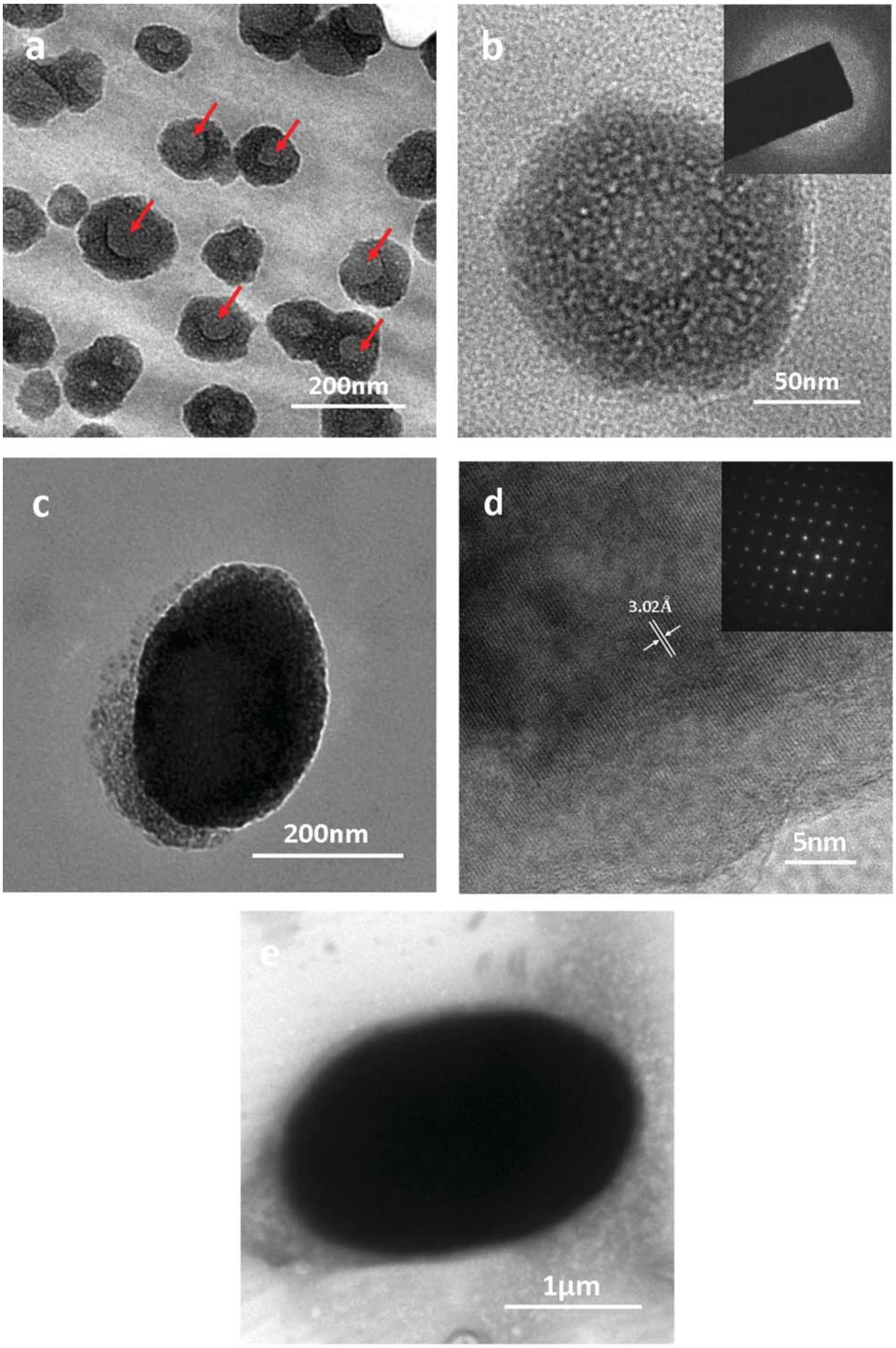

Fig. 2 TEM images of $CaCO_3$ particles obtained under 1 g/l NaCMC and $Ca(OH)_2$ suspension after 10 min reaction (a, b) and after 60 min reaction (c, d), respectively, the red arrows (a) indicates the depression of the particle and the inset of (b)(d) is the ED pattern of the corresponding particle on the image. TEM images of $CaCO_3$ particles obtained under 10 g/l after 60 min reaction (e).

and the size is a little larger than those obtained with 1 g/l NaCMC. The concentration of NaCMC with a larger molecular weight between 1 g/l and 5 g/l in the starting solution had no obvious effect on the size of the $CaCO_3$ particles, suggesting that the concentration is not decisive of the size of particles because the two concentrations are all much larger than the overlapped concentration.

Effect of CO_2 pressure and temperature

We also compared the effects of different pressure and temperature of CO_2.$CaCO_3$ particles were synthesized in 8 MPa and 45 °C CO_2 (supercritical CO_2) under the otherwise same conditions. Fig. 4e–g show the SEM images of particles obtained in $scCO_2$ at 0.1, 1 and 10 g/l NaCMC concentration (M_w of

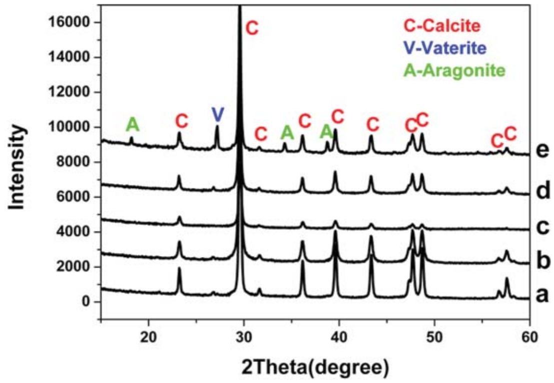

Fig. 3 X-ray diffraction patterns of products obtained under 0.1 g/l(a), 10 g/l(b), 1 g/l(d) NaCMC and $Ca(OH)_2$ suspension after 60 min reaction and products obtained under 1 g/l(c) NaCMC and $Ca(OH)_2$ suspension after 10 min reaction in compressed CO_2; X-ray diffraction patterns of products obtained under 1 g/l(e) NaCMC and $Ca(OH)_2$ suspension after 60 min reaction in $scCO_2$. "C" denotes for the calcite phase (JCPDS86-2334), "V" denotes for the vaterite phase (JCPDS33-0268) and "A" denotes for the aragonite phase (JCPDS71-2392).

90 000), respectively. We find that the morphology and size of the particles is almost the same as those synthesized under compressed CO_2, also the trend of variation of the particles with the varied concentration. That is, the morphology is also ellipsoidal and the size is several hundreds of nanometres. In our reaction system, the decisive factor affecting the reaction is the solubility of CO_2 in water rather than whether the CO_2 condition is compressed or supercritical. According to Diamond and Akinfiev,[27] the solubility of CO_2 in water under our two conditions (20 °C, 5 MPa and 45 °C, 8 MPa) is close. So it is understandable that the particles obtained under two conditions showed little difference. In Han's work,[10] little difference exhibited within the products yielding under the different CO_2 pressures. The XRD patterns depict mainly calcite diffraction peaks and a little fraction of vaterite and aragonite ones, which we suppose is mainly due to the influence of temperature.[28] The content of organic additives is about 6% (see supporting information, Fig. S4, ESI†), which is equal to that obtained under the corresponding conditions in the compressed CO_2. In summary, the effect of CO_2 pressure and temperature was not so obvious.

Verification of the formation mechanism with flexible chain-PAA

To verify the mechanism we suggested that the morphology is determined by the flexibility of the polymer chain, we picked polyacrylic acid (PAA) to perform the contrast experiments. PAA was intensively studied as a model compound about the effect on $CaCO_3$ crystallization.[29-32] Compared to NaCMC chains, the conformation of PAA chain in aqueous solution is much more flexible.[33]

The electron microscope pictures are presented in Fig. 5. Fig. 5a and 5b show the $CaCO_3$ particles obtained under 0.1 g/l PAA and 3 g/l $Ca(OH)_2$ suspension. The particles are spherical with a size of 300–500 nm, and the size distribution is not well dispersed. The rough surfaces of the spheres are due to the coated gold grains when SEM is performed. When the concentration of PAA increased to 1 g/l, the morphology and size of the $CaCO_3$ particles undergoes little change, which are still spherical in size of 300–500 nm (Fig. 5c). The TEM images in Fig. 5d confirmed the morphology and size observed in SEM images and the ED patterns show that the particles are vaterite. As we have mentioned above, the conformation of the PAA chain in aqueous solution is flexible. According to the mechanism we proposed above, it is the flexibility of the polymer chain that determines the final morphology of the particles. So it is easy to understand that $CaCO_3$ grains grew along the PAA coils and thus formed the spherical particles. The results of PAA experiments suggested that the mechanism is efficient.

Overall scheme

Based on the above results, we pictured the formation process of $CaCO_3$ particles in compressed and supercritical CO_2, as the Scheme 1 depicts. The flexibility of polymers determines the final morphology of the particles. For rigid polymer chains (like NaCMC), when the concentration is relatively low, the submicroscopic ellipsoidal particles yield, with a probable ACC intermediate phase during the formation process of the particles; when the concentration is high, the polymer chains overlapped severely, inducing particles with larger size and slightly different morphologies. For flexible polymer chains (like PAA), spherical particles yield. According to such mechanisms, the polymer chains act as the skeletons of the particles, followed by the attachment of ions and growth of $CaCO_3$ grains and the whole organic–inorganic aggregates are constructed.

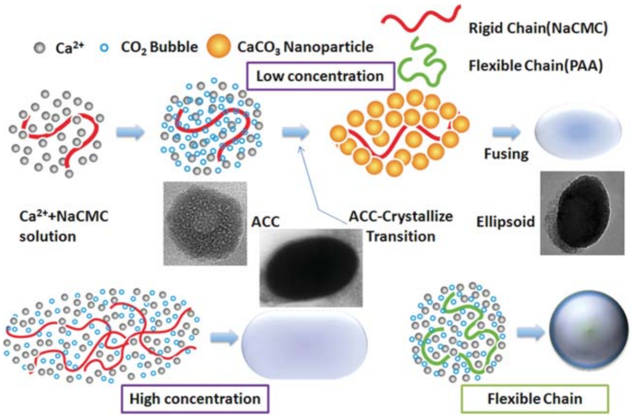

Scheme 1 Schematic illustration of the mineralization mechanism. The relative size of the different species present in solution is not drawn to scale. The polymer chains are the skeletons of the particles and the species attach and grow along the chains, thus the whole organic–inorganic aggregates are constructed. The flexibility of polymers determines the final morphology of the particles. See the text for more details.

We have obtained rosette-like $CaCO_3$ particles with the traditional CO_2-dispersed method.[23] In comparison to the previous results, we find that there is an obvious difference in the mineralization mechanism between the two mineralization methods. There are two features resulted from the high concentration of CO_2 in the present system: fast reaction and homogeneous distribution in the reaction system. The former factor implies that the reaction could be near to completion within short

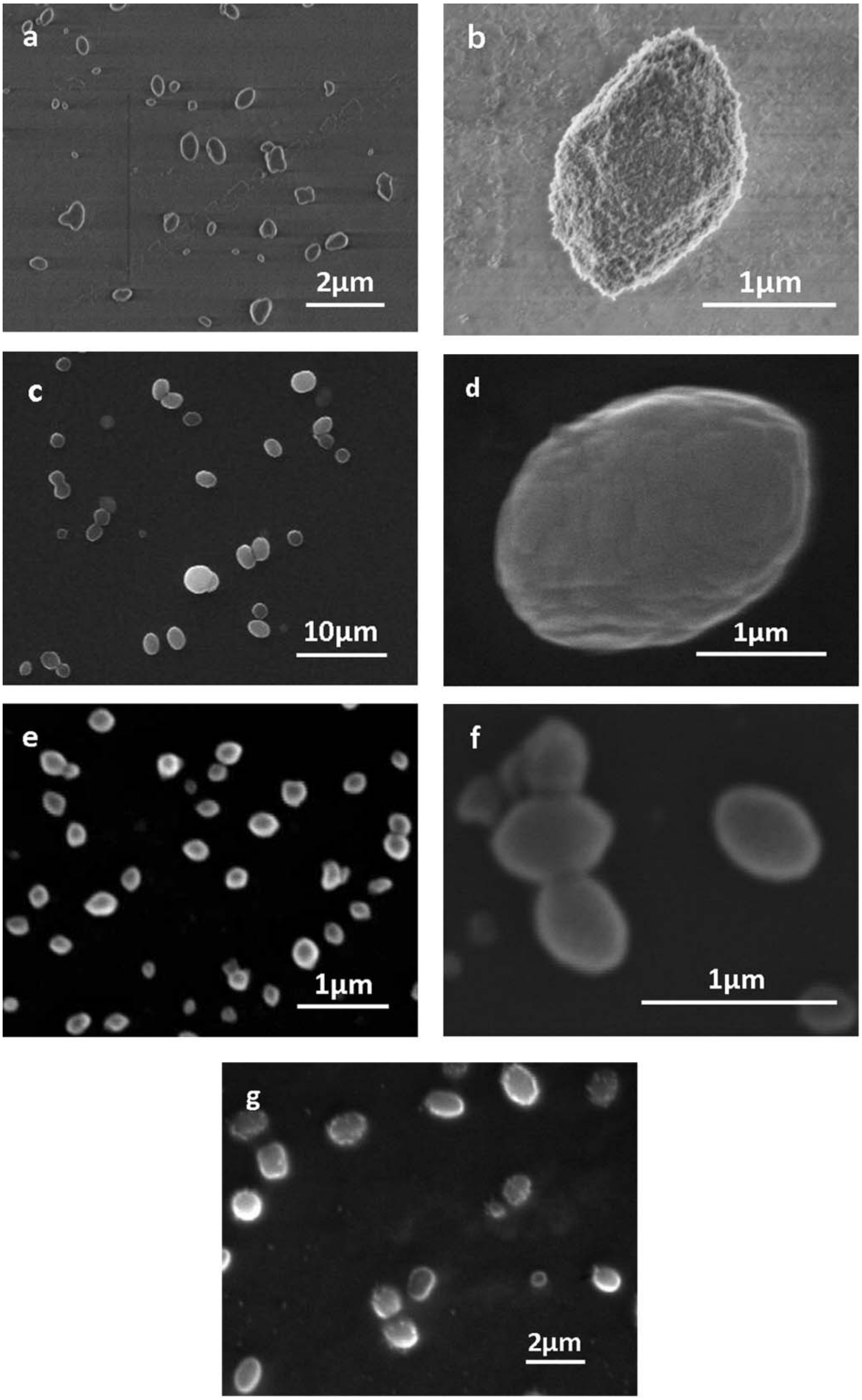

Fig. 4 SEM images of $CaCO_3$ particles obtained under control of NaCMC with a molecular weight of 700 000 in compressed CO_2 at a concentration of 1 g/l (a,b) and 5 g/l (c,d), respectively. SEM images of $CaCO_3$ particles obtained under control of NaCMC with a molecular weight of 90 000 in $scCO_2$ at a concentration of 0.1 g/l (e), 1 g/l(f) and 10 g/l(g).

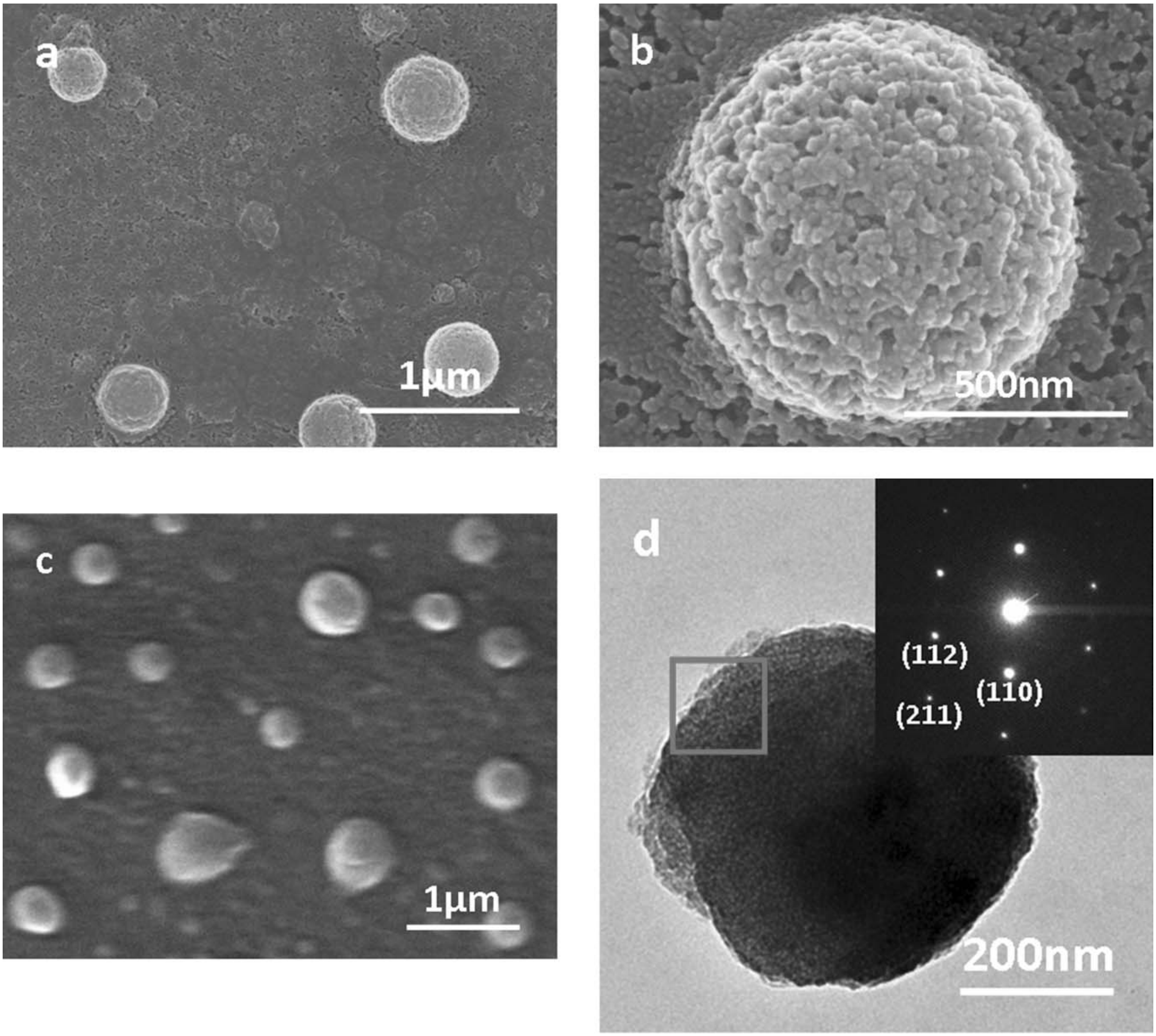

Fig. 5 SEM images of $CaCO_3$ particles under control of 0.1 g/l(a, b), 1 g/l(c) PAA and $Ca(OH)_2$ suspension in compressed CO_2. TEM images of $CaCO_3$ particles under control of 1 g/l (d) PAA and $Ca(OH)_2$ suspension and the inset is ED patterns corresponded to the area the red pane indicates.

interval, the latter one implies that the reaction in any position of the system is the same. In contrast, with the CO_2-dispersed method, the slow diffusion of CO_2 ensures slow nucleation and growth rate of $CaCO_3$ particles and the regularity and size of the particles can be increased in a longer interval. The consequence is that the particles obtained in two conditions show obvious difference in morphology and size.

Conclusions

We have successfully synthesized submicroscopic ellipsoidal calcite particles with a size of several hundreds of nanometres by the use of compressed and supercritical CO_2. By altering the experimental parameters including polymer concentration and chain length of polymer, we can effectively control the morphology and size of the particles. The crystallization mechanism suggested that the polymer chains act as the skeletons, followed by the attachment of ions and growth of $CaCO_3$ grains and the whole organic–inorganic aggregates are constructed. The flexibility of polymers determines the final morphology of the particles. Besides, during the experiment, we seize ACC intermediate, probably as the precursor of the final crystalline phase. Finally, we compare the present method to the traditional CO_2-diffused method, finding that the two features (fast reaction and homogeneous distribution in the system) of the present method yields small-size and relatively irregular particles. Due to the convenience, low-cost and rapid reaction of the present method, we demonstrate here principally a new method to fabricate submicroscopic calcite particles that may be utilized in many industrial aspects. Furthermore, it is also probably an inspiration to the study of the mechanism of biomimetic mineralization.

Acknowledgements

The authors gratefully acknowledge the financial support by the National Science of Foundation of China (NSFC) (Nos. 20774022), the "Leading Scientist" Project of Shanghai (No. 07XD14002), the National Basic Research Program of China (2005CB623800, 2009CB930000) and Open Project Program of the State Key Laboratory of Chemical Engineering, East China University of Science and Technology (HF08001).

References

1 G. Montes-Hernandez, F. Renard, N. Geoffroy, L. Charlet and J. Pironon, *J. Cryst. Growth*, 2007, **308**, 228–236.
2 S. Mann, *Biomineralization Principles and Concepts in Bioinorganic Materials Chemistry*, Oxford University Press, Oxford, 2001.
3 C. Domingo, E. Loste, J. Gomez-Morales, J. Garcia-Carmona and J. Fraile, *J. Supercrit. Fluids*, 2006, **36**, 202–215.
4 C. Domingo, J. Garcia-Carmona, E. Loste, A. Fanovich, J. Fraile and J. Gomez-Morales, *J. Cryst. Growth*, 2004, **271**, 268–273.
5 S. Weiner, I. Sagi and L. Addadi, *Science*, 2005, **309**, 1027–1028.
6 R. J. Park and F. C. Meldrum, *J. Mater. Chem.*, 2004, **14**, 2291–2296.
7 L. Addadi, S. Raz and S. Weiner, *Adv. Mater.*, 2003, **15**, 959–970.
8 H. Wakayama, S. R. Hall and S. Mann, *J. Mater. Chem.*, 2005, **15**, 1134–1136.
9 W. Gu, D. W. Bousfield and C. P. Tripp, *J. Mater. Chem.*, 2006, **16**, 3312–3317.
10 C. X. Zhang, J. L. Zhang, X. Y. Feng, W. Li, Y. J. Zhao and B. X. Han, *Colloids Surf., A*, 2008, **324**, 167–170.
11 D. L. Tomasko, H. B. Li, D. H. Liu, X. M. Han, M. J. Wingert, L. J. Lee and K. W. Koelling, *Ind. Eng. Chem. Res.*, 2003, **42**, 6431–6456.
12 G. S. Tong, T. Liu, G. H. Hu, L. Zhao and W. K. Yuan, *J. Supercrit. Fluids*, 2007, **43**, 64–73.
13 P. Vitoux, T. Tassaing, F. Cansell, S. Marre and C. Aymonier, *J. Phys. Chem. B*, 2009, **113**, 897–905.
14 Q. S. Yu, P. Y. Wu, P. Xu, L. Li, T. Liu and L. Zhao, *Green Chem.*, 2008, **10**, 1061–1067.
15 L. Li, T. Liu, L. Zhao and W. K. Yuan, *Macromolecules*, 2009, **42**, 2286–2290.
16 H. Wakayama, S. R. Hall, Y. Fukushima and S. Mann, *Ind. Eng. Chem. Res.*, 2006, **45**, 3332–3334.
17 F. Cansell and C. Aymonier, *J. Supercrit. Fluids*, 2009, **47**, 508–516.
18 S. Moisan, V. Martinez, P. Weisbecker, F. Cansell, S. Mecking and C. Aymonier, *J. Am. Chem. Soc.*, 2007, **129**, 10602–10606.
19 J. W. Wang, Y. D. Xia, W. X. Wang, M. Poliakoff and R. Mokaya, *J. Mater. Chem.*, 2006, **16**, 1751–1756.
20 J. W. Wang, Y. D. Xia, W. X. Wang, R. Mokaya and M. Poliakoff, *Chem. Commun.*, 2005, 210–212.
21 H. Ohde, J. M. Rodriguez, X. R. Ye and C. M. Wai, *Chem. Commun.*, 2000, 2353–2354.
22 H. Ohde, M. Ohde, F. Bailey, H. Kim and C. M. Wai, *Nano Lett.*, 2002, **2**, 721–724.
23 W. Li and P. Wu, *CrystEngComm*, 2009, DOI: 10.1039/b901580a.
24 A. W. Xu, W. F. Dong, M. Antonietti and H. Colfen, *Adv. Funct. Mater.*, 2008, **18**, 1307–1313.
25 R. Q. Song, A. W. Xu, M. Antonietti and H. Colfen, *Angew. Chem., Int. Ed.*, 2009, **48**, 395–399.
26 K. Kamburova and T. Radeva, *J. Colloid Interface Sci.*, 2007, **313**, 398–404.
27 L. W. Diamond and N. N. Akinfiev, *Fluid Phase Equilib.*, 2003, **208**, 265–290.
28 X. Q. An and C. B. Cao, *J. Phys. Chem. C*, 2008, **112**, 15844–15849.
29 J. G. Yu, M. Lei, B. Cheng and X. J. Zhao, *J. Solid State Chem.*, 2004, **177**, 681–689.
30 T. Miura, A. Kotachi, Y. Oaki and H. Imai, *Cryst. Growth Des.*, 2006, **6**, 612–615.
31 A. Kotachi, T. Miura and H. Imai, *Cryst. Growth Des.*, 2006, **6**, 1636–1641.
32 Q. F. Yang, A. Z. Gu, Y. Q. Liu, H. R. Zeng, J. Ding and Z. Q. Shen, *J. Inorg. Mater.*, 2002, **17**, 559–565.
33 Y. Mylonas, G. Staikos and M. Ullner, *Polymer*, 1999, **40**, 6841–6847.